CCLRC DARESBURY LABORATORY
EPSRC NATIONAL CHEMICAL DATABASE SERVICE

RESEARCH HIGHLIGHTS ASSOCIATED WITH ANNUAL REPORT 2005/6

1. Rational Design of Molecularly Imprinted Polymers - Dr K. Karim:
Cranfield Biotechnology Centre, Cranfield University at Silsoe

2. Modelling for Coordination Complexes: Structure - Guided Force Field Design - Dr R.J. Deeth:
Department of Chemistry, University of Warwick

3. Computer simulations of defects and impurities in natural apatite materials - Drs N.H. de Leeuw & J.A.L. Rabone:
Department of Chemistry University College London and School of Crystallography Birkbeck College London

4. Density measurements through the Main (L_{α} - $P_{\beta'}$) and "Pre" ($P_{\beta'}$ - $L_{\beta'}$) Phase transitions of di-hexadecanoyl-phosphatidylcholine - J. Jones, Drs L. Lue & A. Saiani & Prof. G.J.T. Tiddy:
Department of Chemical Engineering, University of Manchester

5. New anode materials for Li-rechargeable Batteries - Dr M.V. Koudriachova & Prof. N.M. Harrison:
Davy Faraday Research Laboratory, the Royal Institution of Great Britain and CSE Department, CCLRC Daresbury Laboratory

6. The synthesis of indanones related to combretastatin A-4 *via* microwave-assisted Nazarov cyclization of chalcones - Prof. N.J. Lawrence, Prof. A.T. McGown & Dr S. Ducki:
H Lee Moffitt Cancer Center, Tampa, Florida and Centre for Molecular Drug Design, University of Salford

7. A New Class of Asymmetric Ketone Hydrogenation Catalysts – Prof. M. Wills:
Department of Chemistry, University of Warwick

The Archive for the full collection of Research Highlights since 1999 is available at the address: http://cds.dl.ac.uk/report/res_high.html

Rational Design of Molecularly Imprinted Polymers - Kal Karim (k.karim@cranfield.ac.uk)

Cranfield Biotechnology Centre, Cranfield University at Silsoe

Introduction

Our present research is the development of a general method for the rational design of Molecularly Imprinted Polymers (MIPs). Using molecular modelling & computer simulation it is possible to predict & tailor the polymer properties for specific applications. Areas of applicability include drug discovery, detection of toxins/environmental pollutants, both natural & industrial, sensors & assays, separation & in drug development. MIPs have been previously synthesised with high selectivity sensitivity for target compounds such as triazine herbicides, pesticides, algal and fungal toxins, explosives, peptides and a variety of drugs. Their synthesis is via straightforward and inexpensive procedures.

Current Work

Our research has allowed the predictive design of polymer specificity & affinity, new synthetic ligands, further development in the chemistry of conjugated polymers (PANI & polythiophenes) & the ability to incorporate them into transducers such as QCM, SPR, optical & electrochemical detection methods.

We have expanded our monomer database library which we use to screen and select possible monomer candidates for polymer preparation by searching for commercially available functional monomers which are polymerisable but have the necessary substituents to form a complex with a given target. The expansion of the library for virtual screening is a direct result of searching monomers using the MDL Available Chemicals Directory, to which we have ready access via the EPSRC Chemical Database Service (CDS). 3D structures can then be generated using Molecular Mechanics and Molecular Dynamics simulations.

Cranfield Health has a newly acquired multinuclear NMR spectrometer able to investigate samples in both solid and solution phase. This is part of the Science Research Investment Fund (SRIF) and will ensure that novel monomers can be synthesised for many applications. Access to the wide range of reaction databases also available via the CDS allows us to design compounds via viable, cost effective synthetic routes. The main targets are novel multifunctional monomers, which will act as superior monomer candidates for polymer preparation to those currently available, and crosslinkers, which can further enhance the stability of the monomer-template complex. In some cases it may be possible to make polymers with specificity and affinity from these novel multidentate monomers where the template is not required.

A schematic representation of the Molecular Imprinting Polymerisation process

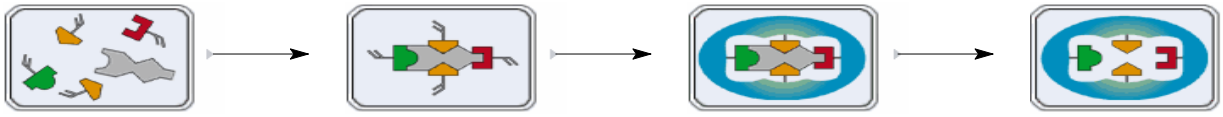

a. Selection b. Self-Assembly c. Polymerisation d. Extraction

Addition Role of the CDS

In addition the CDS has supported our Bioinformatics masters course since its inception 4 years ago, specifically in helping run the "Molecular Modelling and Chemoinformatics" module with great success (giving lectures and running practical sessions).

Modelling for Coordination Complexes: Structure - Guided Force Field Design - Rob Deeth (R.J.Deeth@warwick.ac.uk)

Department of Chemistry, University of Warwick

Introduction

Computer modelling of molecular systems has made impressive progress in recent years and has become firmly established as a discipline in its own right. However, among the many ongoing challenges is the issue of accurately calculating the structures and properties of systems containing transition metals. Compared to the organic chemistry of carbon, the chemistry of a typical transition metal is far more difficult to treat theoretically. The problems include low-lying excited states, complex magnetic properties, high coordination numbers, relatively weak bonds, flexibility, variable oxidation states, and so on. One way forward is to model the system using quantum mechanics (QM) and the advent of Density Functional Theory (DFT) has been a huge boon. However, all QM methods are compute intensive and it may not be possible to get a sufficiently accurate answer in a reasonable amount of computer time.

Dealing with large organic systems using QM is similarly problematic but here, researchers have resorted to simpler models based on classical mechanics. In essence, the true quantum nature of molecules is replaced by a 'ball-and-spring' picture called molecular mechanics (MM). Although apparently unsophisticated compared to QM, MM can be a remarkably good way of modelling molecules, especially those based on carbon chemistry, because carbon behaves in clear, well-defined ways which are relatively simple to capture mathematically.

For example, each carbon atom is connected to four, three or two other atoms with well-defined geometries – tetrahedral, trigonal and linear respectively (Figure 1). In each case, the angles subtended at the carbon are the same – 109.5, 120 and 180° respectively. It is this geometrical simplicity which allows the ball-and-spring approach to work well and since simple classical equations are used for the so called force field (FF) which describes bond stretching, angle bending, torsional twisting and non-bonding interactions (van der Waals and electrostatics), MM is extremely fast.

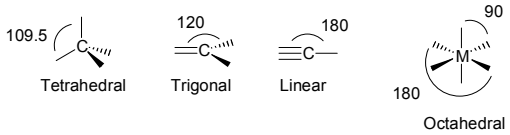

Figure 1 - Ideal geometries for carbon and the octahedral structure typical in TM chemistry

However, TM complexes are more complicated. A very common structure in TM chemistry is the octahedron (Figure 1 right) which already causes problems since now there are two possible 'ideal' angles at the metal – 90 or 180° – but the L-M-L triad is the same.

A simple remedy to this problem is to look at a model like valence shell electron pair repulsion (VSEPR) theory covered in most first year undergraduate chemistry courses. Here, the basic structure around a central atom is determined by the mutual repulsions of bond pairs and lone pairs. Thus, six groups around a central metal will automatically arrange themselves into an octahedron. The necessary interaction can be conveniently treated via a points-on-a-sphere (POS) scheme.

However, many TM species do not obey VSEPR predictions. Superimposed on the desire of ligands to get as far from each other as possible is an electronic effect arising from the metal's d electrons. The ligands around the metal split the d orbitals into characteristic patterns relative to the energy zero or barycentre. Electrons going into orbitals lower than the barycentre stabilise the system while those going into high energy orbitals destabilise it.

For a four-coordinate system, this stabilisation energy is a maximum at the planar limit but the ligand-ligand repulsion favours the tetrahedron. If the electronic stabilisation is relatively weak, a tetrahedral geometry results ($[NiCl_4]^{2-}$) but if it is strong, a planar geometry results ($[Ni(CN)_4]^{2-}$). If the balance is more equal, an intermediate structure is found ($[CuCl_4]^{2-}$). Clearly, any theoretical model must explicitly or implicitly account for these electronic effects.

Results

A simple yet powerful method for treating d electron effects is ligand field theory (LFT). LFT derives from the earlier crystal field model introduced by Bethe in 1929 and involves parameterising the d orbital energies with respect to the surrounding ligands. Given its empirical nature, LFT calculations are very fast compared to QM and thus ideally suited to molecular mechanics. Thus, we have extended conventional MM by adding an explicit calculation of the d electronic stabilisation energy based on generalised LFT – ligand field molecular mechanics (LFMM).

Complexes of the Cu^{2+} ion provide a stringent test of the utility of the LFMM approach. The d^9 electronic configuration is associated with pronounced structural changes. Perhaps the most famous is the large tetragonal distortion displayed by $[Cu^{II}L_6]$ species and generally attributed to the Jahn-Teller effect. Rigorously octahedral Cu^{2+} complexes possess an orbitally degenerate ^2E_g ground state and, as described by Jahn and Teller, are therefore unstable with respect to molecular vibrations which remove the degeneracy.

Given the vibrational motion shown on the right of Figure 2 the d orbitals split as shown on the left. Since there are two electrons going down in the d_z2 orbital and only one going up in $d_x2_{-y}2$ there is a net electronic stabilisation of ΔE_{JT} driving the distortion. This is countered by the vibrational energy which favours the octahedron, hence the final geometry is a balance between these two competing terms.

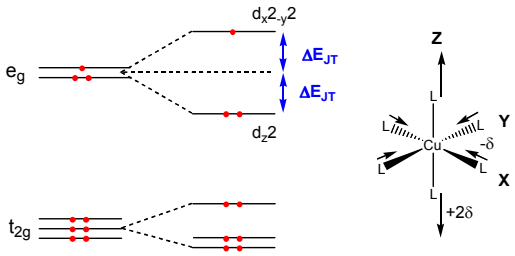

Figure 2 - Schematic representation of the Jahn-Teller effect

QM implicitly treats the Jahn-Teller distortion so we set about finding out whether the LFMM could emulate this behaviour. Being empirical, we needed to develop optimal LFMM FF parameters for describing the stabilisation energy plus Cu-L bond stretching and the L-L non-bonding interactions. Ligand field parameters were derived from previous studies of the electronic spectra of Cu^{II} complexes [1] while the other parameters relied on fitting calculated structures to experimental data.

The Cambridge Structural Database plays a crucial role here as it provides 3-D coordinate data for a large number of Cu^{II} complexes. Since the Jahn-Teller effect is relatively subtle, minor changes in the ligands can result in major changes in the structure. Hence, even though the basic Cu-L interactions are the same – all amines for example – the details of the ligand structure can generate large variations in Cu-L bond lengths. This is a real advantage since a single set of parameters fitted to a diverse range of structures is likely to be very good. In contrast, other metal centres require extensive additional energetic data, usually based on detailed QM calculations.

Based on a training set of 17 molecules downloaded from the Chemical Database Service, LFMM parameters were developed for four-, five- and six-coordinate copper-amine complexes [2]. The root-mean-square error in Cu-N distances was less than 0.02 Å, a significant achievement given that the observed Cu-N distances span the range 1.94 Å through to 2.65 Å.

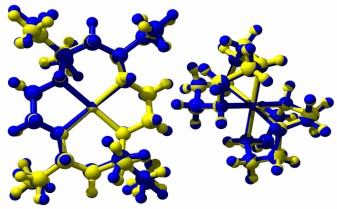

Figure 3 - Overlay of computed (yellow) and observed (blue) structures for some Cu(II) amine complexes

Given the success for simple amine complexes, the LFMM modelling was then extended to treating the full Jahn-Teller effect [3]. Again, structural data from the CSD were crucial to refining the existing, and developing new, parameters.

Moreover, impressive agreement with experiment was obtained (Figure 4). The LFMM has a sufficiently realistic physical basis to generate results of the same quality as full-blown QM treatments, but achieves this performance up to 10000 faster.

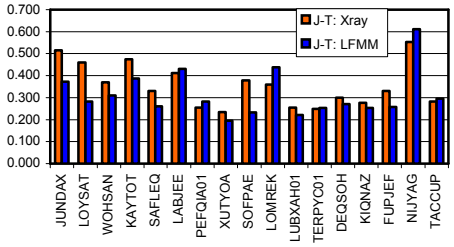

Figure 4 - Experimental and LFMM Jahn-Teller distortions. The bars represent the difference between the averaged equatorial bond length and averaged axial bond length (Å)

The availability of the Chemical Database Service has been of great value during the course of this project. We made use of both the Cambridge ConQuest analysis package as well as the CDS CrystalWeb system. The latter gives us useful linking to the electronic primary literature and easy download facilities for the model structures.

[1] R. J. Deeth and M. Gerloch, *Inorg. Chem.*, 1984, **23**, 3846.
[2] R. J. Deeth and L. J. A. Hearnshaw, *Dalton Trans.*, 2005, 3638.
[3] R. J. Deeth and L. J. A. Hearnshaw, *Dalton Trans.*, 2006, 1092.
Inorganic Computation Chemistry Group website: http://www.warwick.ac.uk/go/iccg

Computer simulations of defects and impurities in natural apatite materials - Nora de Leeuw & Jeremy Rabone (n.h.deleeuw@ucl.ac.uk, j.rabone@mail.cryst.bbk.ac.uk)

Department of Chemistry University College London and School of Crystallography Birkbeck College London

Introduction

Apatites are an abundant and diverse group of minerals that are found in almost all igneous rocks and to a lesser extent in sedimentary and metamorphic rocks. Apatite minerals have a number of important applications, which make them the subject of intensive research:

1. They provide a suitable system for geological thermochronometry through measurements of fission track annealing and helium diffusion, due to radioactive decay in the crystals;
2. Hydroxyapatite is a major constituent of bone and tooth enamel, and is therefore an obvious candidate for bio-compatible artificial bone tissue;
3. Because of their affinity for impurity ions, apatites can sequester heavy metal ions, and may thus provide useful sinks for the immobilisation of heavy metals and radioactive waste.

Most natural apatites, for example, fluorapatite, crystallise in the hexagonal system $P6_3/m$, whereas pure hydroxyapatite and chlorapatite crystallize in the monoclinic system $P2_1/b$. The monoclinic cell is similar to two hexagonal cells arranged along their b-axis and sheared one unit cell along the a-axis, shown in Figure 1. For the sake of convenience, monoclinic apatite crystals may be thought of as having a hexagonal structure with the chloride or hydroxide ion displaced along the principal axis. The general formula of apatite is $A_{10}(PO_4)_6X_2$, where A is usually a divalent cation, commonly calcium, and X is usually F^-, Cl^- or OH^-.

Many variations of the apatite structure exist, and a vast number of substitutions can be made at all of the ion sites. In natural apatites, substitutions tend to be coupled so that, for example, when a trivalent ion replaces a calcium ion, there is either a corresponding substitution of another calcium ion with a univalent ion or one of the anions is replaced by one of a higher valency [1].

Results

We have carried out a computational investigation of a comprehensive range of pure and substituted apatite materials, using the ICSD provided by the Daresbury Chemical Database Service to obtain the structures of the known apatite minerals to develop our models, followed by calculations of the structures and energies of a range of unknown defect structures [2]. Here we present the results of our simulations of solid solutions of calcium and strontium hydroxyapatites.

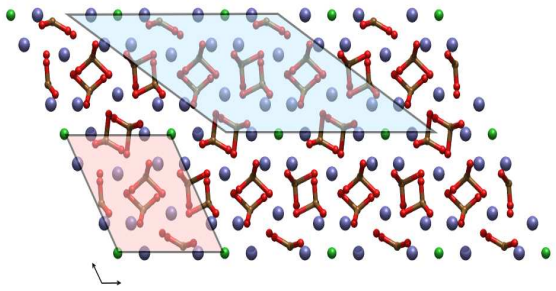

Figure 1. View onto the (0001) plane of the fluorapatite crystal structure, showing the hexagonal symmetry and the relationship between a hexagonal unit cell (pink) and a monoclinic unic cell (blue) (Ca = blue, O = red, P = yellow, F = green).

Strontium apatites form a complete solid solution with calcium apatites [3], where strontium shows a preference for the 6h cation site in the mixed compounds, probably because it is the larger cation, and therefore fits better in the site with a coordination of nine. At high concentrations of strontium the symmetry of hexagonal apatites is reduced from $P6_3/m$ to $P6_3$ because strontium occupies alternating 4f sites. A similar site preference occurs in the monoclinic apatites, such as hydroxyapatite.

We have investigated three strontium calcium hydroxyapatites for which information on site occupancies is available, as shown in **Table 1**. The enthalpies of mixing are calculated by subtracting the enthalpy of formation of stoichiometric amounts of the end members from the enthalpy of formation of the mixed crystal. The statistical ideal entropies of mixing are calculated by assuming that ions in the mixed structure are equally likely to occupy any of the available sites. They are used here only for comparison with the experimental enthalpies of mixing, as they are not necessarily applicable to solids where site preferences exist. The equations in the case of mixed calcium-strontium hydroxyapatites are:

$$\Delta H_{mix} = \Delta H_f [Ca_{x1}Sr_{x2}(PO_4)_6(OH)_2] - (x_1 \times \Delta H_f [Ca_{10}(PO_4)_6(OH)_2] + x_2 \times \Delta H_f[Sr_{10}(PO_4)_6(OH)_2])$$

$$\Delta S_{mix,\ ideal} = -RT \times (x_1 \times \ln[x_1] + x_2 \times \ln[x_2])$$

where x_1 and x_2 are the mol fractions of calcium and strontium, respectively.

Composition	Site	Ca	Sr
$Ca_{8.98}Sr_{1.02}(PO_4)_6(OH)_2$	4f	0.9040	0.0960
	6h	0.8940	0.1060
$Ca_{7.684}Sr_{2.316}(PO_4)_6(OH)_2$	4f	0.8050	0.1950
	6h	0.7440	0.2560
$Ca_{3.616}Sr_{6.384}(PO_4)_6(OH)_2$	4f	0.4630	0.5370
	6h	0.2930	0.7060

Table 1. Site occupancies in calcium-strontium hydroxyapatite [4]

Figure 2 shows the experimental enthalpies of mixing between strontium and calcium hydroxyapatite along with the predicted enthalpies of mixing, where the thick lines with error bars show experimentally determined enthalpies of mixing [3,5]. The green squares show the enthalpies of mixing predicted for structures determined by X-ray diffraction [4,6,7], using a mean field approach in which potentials are scaled according to site occupancy. The lower red lines show the ideal entropies of mixing at 273 K and the upper red lines show the ideal entropies of mixing at 723 K, the temperature at which the mixed apatites were ignited. The dashed and solid blue lines show the enthalpies of mixing predicted by optimizing the pure calcium apatites with explicit substitution by strontium, over a range of compositions.

Two methods were used to predict the lattice enthalpies:

1. A mean field approach in which the potentials of ions are scaled according to site occupancy. In the computer program GULP [8], this means that there is an "averaged" ion at sites with variable occupancy as both of the ions are optimized together. Two dashed lines are plotted on the graphs; the upper one shows the predicted enthalpy of mixing when no site preference is given between the calcium and strontium ions. The lower one shows the situation when strontium preferentially occupies the 6h site or equivalent.
2. A combinatorial approach using discrete replacement of ions in the unit cell. The lattice enthalpies were calculated for each of the 1024 possible combinations of calcium and strontium ions in the 10 cation sites of the unit cell. The graphs show the mixing enthalpies calculated using the maximum (upper blue lines), minimum (lower blue lines), and mean (thick blue lines) lattice enthalpies for each set of combinations.

These methods are only able to provide approximate representations of the crystal structures. In the first method the ion occupations are averaged over the whole structure, which prevents the system from adopting the correct structure when ions possess different radii. Additionally, it was observed that the optimisation procedure did not converge very well and was sensitive to the starting structure. Although the second method does allow proper optimization of defect structures, it has the disadvantage of forcing atoms into a limited number of combinations allowed in the 10 sites of a single unit cell. Although the number of different configurations considered is already large, ideally, all of the possible combinations available for each fraction of strontium would need to be explored. However, for a real crystal this would be almost infinite.

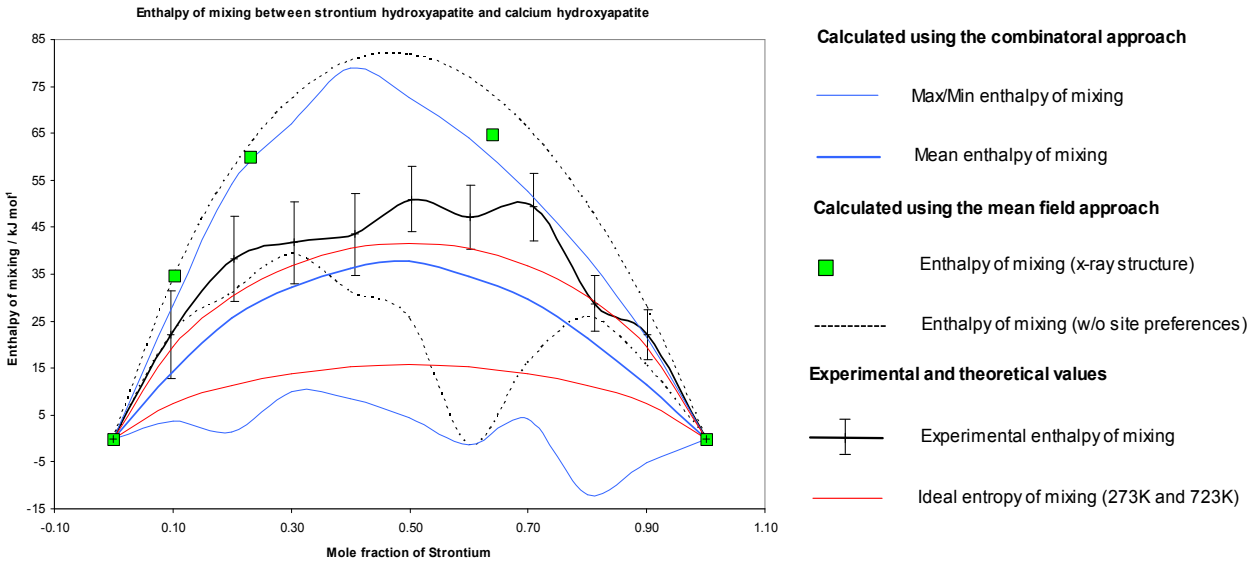

Figure 2. Experimental and predicted enthalpy of mixing curves between strontium and calcium hydroxyapatite.

The mean field method gives reasonable agreement with experiment when experimentally determined structures are used in the optimisation. Starting from an end-member structure and assuming an even distribution of strontium ions, the mixing curve reproduces the correct general trend but underestimates the lattice enthalpy by about 30 kJ mol^{-1} at the midpoint. Using end-member structures, but assuming that strontium preferentially occupies the larger sites, confirms that lower lattice enthalpies can be obtained even though the fit is not very close. The mean field approach is therefore unsuitable, unless the mixed structure is already known, as structures cannot relax fully around the defects.

The combinatorial approach gives good agreement with experiment when the enthalpies for all of the combinations for a given fraction of strontium are averaged. A simple mean does, however, ignore any site preferences, and a more accurate investigation would need to include contributions from many more possible combinations, not just those available in a single, if large, unit cell. The lowest energy structures show small alternations in the enthalpy of mixing with lower energies, when there is an even number of strontium ions in the unit cell. This suggests that the strain caused by replacing a calcium ion with a larger strontium ion can be partially alleviated by replacing a second calcium ion.

A comparison of the experimental mixing curves with calculated ideal entropies of mixing suggest that they represent high temperature mixtures rather than material fully equilibrated at room temperature. If this were the case, then it would not be surprising that the crystals do not adopt the lower energy configurations predicted by the calculations in the combinatorial approach and the averaged curve is closer to reality.

This work has been enabled by the Chemical Databases Service which gives us access to the ICSD. This has provided the known structures of the various apatite phases, which we needed to develop the interatomic potential models for the computer simulations. We have made use of both the CrystalWeb and the ICSD-WWW interfaces. In return, our calculated structures of the solid solutions and other substituted defective apatite materials will become available to the UK community via the Daresbury Chemical Database Service.

[1] J. Barbarand, A. Carter, I. Wood, T. Hurford, *Chem. Geol*. **198**, 107 (2003).
[2] J.A.L. Rabone and N.H. de Leeuw, *J. Comput. Chem*. **27**, 253 (2006).
[3] I. Khattech and M. Jemel, *Thermochim. Acta* **298**, 23 (1997).
[4] A. Bigi, G. Falini, M. Gazzano, N. Roveri and E. Tedesco, *Mater. Sci. Forum* **278**, 814 (1998).
[5] I. Khattech, J.L. Lacout and M. Jemel, *Ann. Chim. Sci. Mater*. **21**, 259 (1996).
[6] J.F. Rakovan and J.M. Hughes, *Can. Miner*. **38**, 839 (2000).
[7] D.Y. Pushcharovskii, T.N. Nadezhina and A.P. Khomyakov, *Kristallografiya* **32**, 891 (1987).
[8] J.D. Gale, *J. Chem. Soc. Faraday Trans*. **94**, 629 (1997).

Density measurements through the Main (L_α - $P_{\beta'}$) and "Pre" ($P_{\beta'}$ - $L_{\beta'}$) Phase transitions of di-hexadecanoyl-phosphatidylcholine - John Jones, Gordon Tiddy, Leo Lue and Alberto Saiani (J.Jones@postgrad.manchester.ac.uk, Gordon.Tiddy@manchester.ac.uk, Leo.Lue@manchester.ac.uk, A.Saiani@manchester.ac.uk)

Department of Chemical Engineering, University of Manchester

Introduction

Lipids are increasingly gaining importance as a basic component of innovative biotechnological and pharmacological applications. It is of little surprise then that lipid bilayers have been much studied as the prototypical membrane. A main focus of such studies is the structure of lipid bilayers and how the lipid bilayer (different makeup of lipids in the bilayer) properties are affected by its environment [1, 2].

The use of density measurement to observe the volume change over the main and pre-transitions is a technique seldom used. However, when coupled with other non evasive techniques, such as calorimetry (microDSC), it becomes a powerful tool that provides some fascinating insights into the phase behaviour of lecithin bilayers. Usually, these observations are used to estimate either the volume of the lipid molecules or the energy associated with a phase transition.

Taking this approach to the next level, we can use the two techniques to calculate volume occupied by each CH_2 group and specific internal energy changes over phase transitions. The energy changes over the main transition can be largely attributed to van der Waals and rotameric energy changes, the sum of which is approximately equal to the enthalpy change of the main transition. Both the volume and energy change per CH_2 group can be estimated by comparison to the volumes and vaporization energies of normal alkanes - utilising the invaluable DETHERM database.

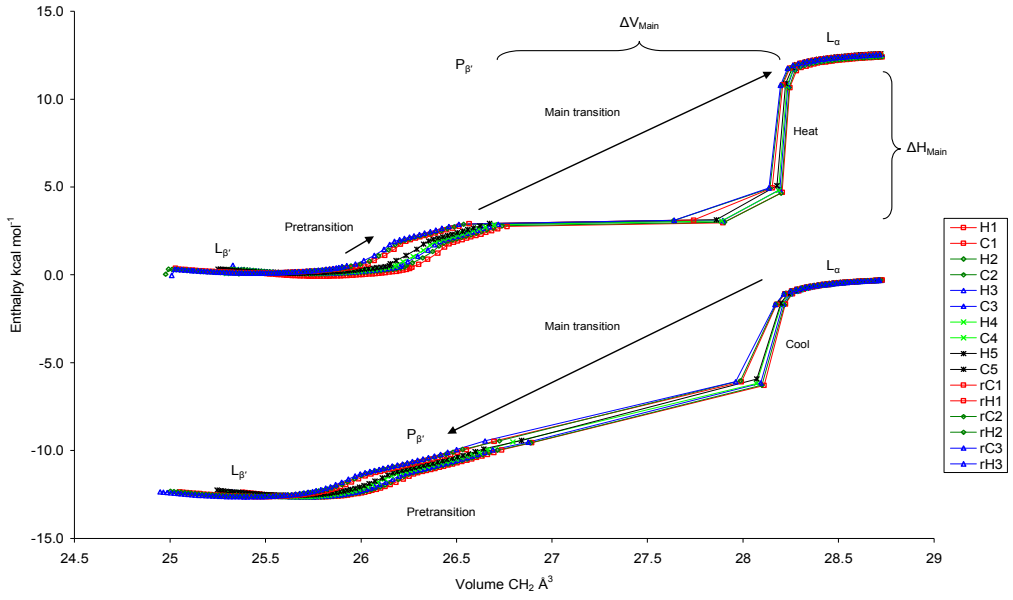

Figure 1 A chart showing enthalpy as a function of CH_2 group volume. The curves show measurements for a sequence of five heat/cool cycles (H1, C1, H2, C2, H3, C3, H4, C4, H5, C5) after initial equilibration at 5°C for 24h. The sample was then held at 50°C for 24h followed by three heat/cool cycles (reC1, reH1, reC2, reH2, reC3, reH3. The volume (ΔV_{Main}) and enthalpy (ΔH_{Main}) change over the main transition are highlighted.

Experiments & Results

Experiments on several lecithins, chiefly di-hexadecanoyl-phosphatidylcholine, have been carried out using the density meter (Anton Paar DMA 5000) and microDSC (Setaram microDSC III) [3] and have revealed a large unreported volume hysteresis phenomenon. By manipulating the volume and microDSC data in this way, it is possible to directly compare the volume and energy changes as a function of temperature and gain some remarkable insights into the mechanism behind the phase transitions.

Some hysteresis in volume per CH_2 group between heating and cooling is clearly visible in Figure 1, existing predominantly in the low temperature gel phase. This phenomenon is believed to be an effect of the continual development of low volume gel phases through successive temperature cycling. Eventually the hysteresis does reach an equilibrium value at which further heat/cool cycling no longer changes the volume. Remarkably, we also observe pretransitional behaviour in the L_α phase before the main transition, suggesting the presence of gel-like lipid patches, as has been found in other research on biological membranes. These appear to result in the formation of a different gel phase on subsequent cooling cycles.

In this analysis, the volume per CH_2 group was found to be in remarkably good agreement with work proposed in Refs. [1, 4] and in computational models [5]. But interestingly, the van der Waals energy change over the main phase transition was found to be smaller than the rotameric energy change; quite the reverse of the results in Ref. [1]. Here again, the DETHERM database has provided invaluable reference data with which detailed theoretical calculations can be performed. Importantly, we can also estimate the van der Waals energies of other molecules provided the volume change per CH_2 group is known.

In the future we plan to investigate the influence of other components (e.g. cholesterol, fatty acids) on these phenomena. We anticipate that having ready access to the DETHERM database as is provided by the EPSRC Chemical Database Service will play a major role in the selection of specific materials.

[1] Nagle, J.F. and D.A. Wilkinson, *Lecithin bilayers. Density measurement and molecular interactions.* Biophysical Journal, 1978. **23**(2): p. 159-173.

[2] Lin, H.N., *Differential scanning calorimetry study of mixed-chain phosphatidylcholines with a common molecular weight identical with diheptadecanoylphosphatidylcholine.* Biochemistry, 1990. **29**: p. 7063-7072.

[3] Jones, J., et al., *Density measurements through the gel and lamellar phase transitions of di-tetradecanoyl- and di-hexadecanoyl-phosphatidylcholines;*

[4] Nagle, J.F. and S. Tristram-Nagle, *Structure of lipid bilayers.* Biochimica Et Biophysica Acta, 2000. **1469**(3): p. 159-95.

[5] Chiu, S.W., et al., *Application of combined Monte Carlo and molecular dynamics method to simulation of dipalmitoyl phosphatidylcholine lipid bilayer.* Journal of Computational Chemistry, 1999. **20**(11): p. 1153-1164.

New anode materials for Li-rechargeable Batteries - Marina Koudriachova & Nicholas Harrison (marina_koudriachova@hotmail.co.uk, n.m.harrison@dl.ac.uk)

Davy Faraday Research Laboratory the Royal Institution of Great Britain and CSE Department CCLRC Daresbury Laboratory

The efficient production and storage of energy from renewable sources requires the development of new materials with highly optimised properties. Li-rechargeable batteries are efficient energy storage devices providing high energy density and are capable of both high voltage and power. Practical electrode materials must have the ability to take up and release lithium ions during many charge and discharge cycles.

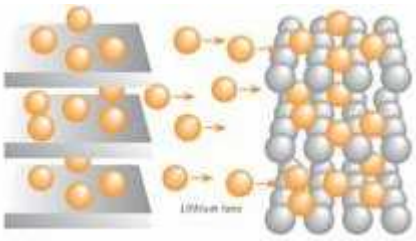

Principle of functioning of a Li-electrochemical cell. In the state of the art Li-batteries both, anode and cathode, are transition metal oxide based material

For the battery performance the following factors are important: the voltage difference between the electrodes, how many lithium ions can be accommodated, the rate of intercalation and the number of charge discharge cycles before the electrodes degrade. Intercalation at a constant potential is preferable – with a low potential required for the anode and a high potential for the cathode. The contradictory requirements of high energy density, stable structure (for cyclability) and rapid diffusion (for high current) mean that the development of new materials requires a detailed understanding of the intercalation mechanism.

Titanium dioxide based materials are among the few which can intercalate Li-ions at a low potential and are therefore promising anode materials. In addition they are easily accessible, chemically stable, relatively inexpensive and environmental friendly. Titania also exists in a number of TiO_2 polymorphs, which can be readily prepared in nano-crystalline form with high surface area and low density.

Different titania morphologies exhibit a strikingly different intercalation behaviour. Two of the polymorphs - anatase structured TiO_2 and spinel structured Li-titanates - are currently used as anode materials in commercial batteries as they intercalate Li at a constant potential and show remarkable cyclability. However, their Li-intercalation potential is too high for some applications. The current challenge is to identify morphologies and to optimize its properties.

Computer simulations based on quantum mechanics allow one to study the properties of known polymorphs in order to establish their suitability as electrode materials in Li-batteries. Connecting to the Inorganic Crystal Structures Database provided by the Chemical Database Service using the DLVisualize software [1] we have identified a number of prospective structures and investigated their intercalation behaviour [2-5].

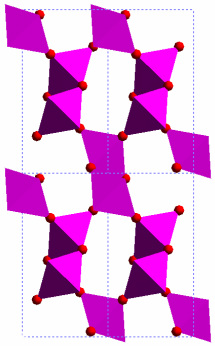

An example of such a material is TiO_2 with the ramsdellite structure (see above), which is predicted to intercalate Li-ions through a two phase equilibrium at the lowest intercalation potential achieved so far for Li-titanates – about 0.3 eV lower than that for spinel structured Li-titanates [6].

[1] DLVisualize: B.G. Searle, Computer Physics Communications, 137, p. 25 (2001) http://www.cse.clrc.ac.uk/cmg/DLV/
[2] M.V.Koudriachova, N.M.Harrison, S.W. de Leeuw, Phys.Rev. **B 65**, 235423 (2002)
[3] M.V.Koudriachova, N.M.Harrison, S.W. de Leeuw, Chem.Phys.Lett**. 371**, 150 (2003)
[4] M.V.Koudriachova, N.M.Harrison, S.W. de Leeuw, Phys. Rev. **B 69**, 54106 (2004)
[5] M.V.Koudriachova, N.M.Harrison, Mater. Chem., 2006, 16, 1973 – 1977 (2006)
[6] M.V.Koudriachova, N.M.Harrison, in preparation

The synthesis of indanones related to combretastatin A-4 *via* microwave-assisted Nazarov cyclization of chalcones – Nicholas Lawrence, Alan McGown, Sylvie Ducki (LawrenNJ@moffitt.usf.edu, mcgown@salford.ac.uk, s.ducki@salford.ac.uk)

H Lee Moffitt Cancer Center, Tampa, Florida and Centre for Molecular Drug Design, University of Salford

Our research groups have a long-standing interest in anticancer agents, especially those derived from natural products. In 1996, as part of a plant-screening program, we identified *Scutellaria barbata* D. Don (*Labiatae*) as a potential source of anticancer agents. The dried whole plant, readily available from herb wholesalers, is used in traditional Chinese medicine as an anti-inflammatory and antitumour agent. It is a component of Shan Ci Gu soup, a herbal prescription for stomach cancer.

Bioassay guided fractionation of the herb extract, using the MTT assay to determine cytotoxicity, revealed the presence of many cytotoxic components. One such fraction had an IC_{50} (K562) of 10 µg/mL. The fraction was predominantly the simple enone **1** (IC_{50} 60 µM) [1]. Preparation of a library of butenones revealed that those possessing electron-withdrawing groups were the most active [2] The pentafluorophenylbutenone **2** was over 30 times more active than the natural product **1**.

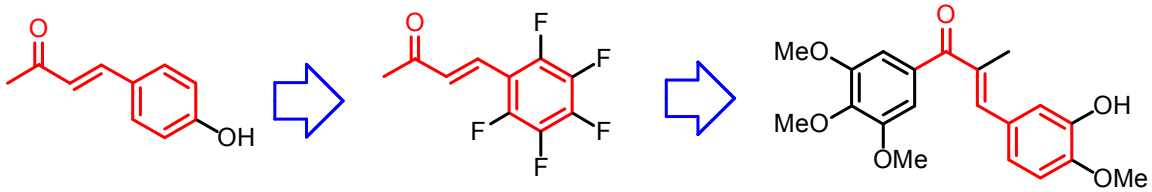

1, IC_{50} (K562) 60 µM **2**, IC_{50} (K562) 1.9 µM **3**, IC_{50} (K562) 0.2 nM

The activity appears to be associated with ability to act as an alkylating agent. Further structural modification and library design [3] led to discovery of the alpha-methylchalcone **3**, which operates biologically by a different mechanism [4]. This chalcone shows potent cytotoxicity, and inhibits cell growth, over a period of several days, by binding strongly to tubulin, a protein essential for cell division [5]. Perhaps more exciting is its ability to cause selective damage to tumor vasculature in a matter of minutes. This effect is also thought to be related to its tubulin binding property. In this way tumors are starved of oxygen and nutrients and their constituent cells die. Compounds such as these that target tumor vasculature clearly have significant clinical promise for the treatment of cancer.

As part of a recent study to determine the features of the chalcone that lead to good biological activity we have developed a fast and efficient microwave-assisted synthesis of indanones [6]. Microwave irradiation provides a useful alternative to traditional heating techniques to promote the trifluoroacetic acid (TFA) catalyzed Nazarov cyclization of chalcones.

The use of the microwave reactor is ideal for handling potentially hazardous reagents such as TFA. The reactions can be performed quickly, conveniently and safely: both the temperature and the pressure of the reaction vial are monitored continuously. The exposure to pressurized reaction vessels containing TFA is thereby significantly reduced.

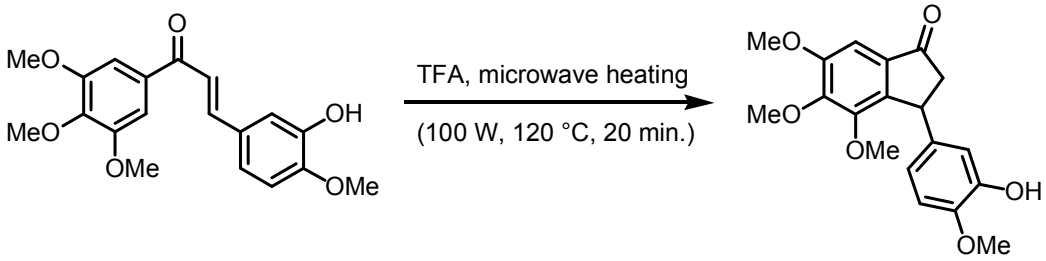

Throughout the study we have made frequent use of the CDS. Specinfo was useful for assigning structures of the natural products derived from the herbs. Structural and activity analysis of products was also helped by access to the Cambridge Crystallographic database. We made regular use of the CDS reaction databases with particular emphasis on the various 'specialist' systems including SPS (solid phase synthesis) and Chirbase (chiral separation by chromatography). The Available Chemical Directory is very useful for quickly sourcing starting materials and building blocks for library design. In summary our research has been greatly aided by our access to the Service.

1. Ducki, S.; Hadfield, J. A.; Lawrence, N. J.; Liu, C. Y.; McGown, A. T.; Zhang, X. G., Isolation of E-1-(4'-hydroxyphenyl)-but-1-en-3-one from Scutellaria barbata. *Planta Medica* **1996,** 62, 185-186.
2. Ducki, S.; Hadfield, J. A.; Hepworth, L. A.; Lawrence, N. J.; Liu, C. Y.; McGown, A. T., Synthesis and cell growth inhibitory properties of substituted (E)-1-phenylbut-1-en-3-ones. *Bioorg. Med.Chem. Lett.* **1997,** 7, 3091-3094.
3. Lawrence, N. J.; Rennison, D.; McGown, A. T.; Ducki, S.; Gul, L. A.; Hadfield, J. A.; Khan, N., Linked Parallel Synthesis and MTT Bioassay Screening of Substituted Chalcones. *J. Combi.Chem.* **2001,** 3, 421-426.
4. Ducki, S.; Forrest, R.; Hadfield, J. A.; Kendall, A.; Lawrence, N. J.; McGown, A. T.; Rennison, D., Potent antimitotic and cell growth inhibitory properties of substituted chalcones. *Bioorg. Med. Chem. Lett.* **1998,** 8, 1051-1056.
5. Lawrence, N. J.; McGown, A. T.; Ducki, S.; Hadfield, J. A., The interaction of chalcones with tubulin. *Anti-Cancer Drug Design* **2000,** 15, 135-141.
6. Lawrence, N. J.; Armitage, E. S. M.; Greedy, B.; Cook, D.; Ducki, S.; McGown, A. T., The synthesis of indanones related to combretastatin A-4 via microwave-assisted Nazarov cyclization of chalcones. *Tetrahedron Lett.* **2006,** 47, 1637-1640.

A New Class of Asymmetric Ketone Hydrogenation Catalysts - Martin Wills (m.wills@warwick.ac.uk)

Department of Chemistry, University of Warwick.
Financial Support from EPSRC, BBSRC, Astrazeneca, Pfizer, GlaxoSmithKline, Rhodia, EvotecOAI, Avecia, the Foreign and Commonwealth Office, the Royal Society, Arran Chemicals, Kao Corporation, Ajinomoto, Johnson Matthey and Dow chemicals.

Introduction

As all chemists will be aware, the ability of large numbers of molecules to exist in two non-superimposable, mirror-image forms (or enaniomers) is an issue of major significance not only the very existence of life but also to researchers in the pharmaceutical, agrochemical and fine chemical industries. Since two enantiomers may have dramatically different physiological effects, it is essential that methods are available for the preparation of single enantiomers in high yield and purity when required. Of the many methods available, the most desirable method is the use of a catalyst to induce the required chirality at a key step, using a relatively readily available and inexpensive primary reagent. In contrast to resolution and stoichiometric methods, asymmetric catalysis offers significant environmental as well as cost and handling benefits, because fewer side products are formed, less energy is required, and solvent quantities are minimised. Asymmetric synthesis and, particularly asymmetric catalysis, is now a multi-billion dollar research area under investigation in industrial and academic laboratories throughout the world.

One of the most pivotal methods for the preparation of chiral molecules by asymmetric catalysis is the reduction of a ketone to an enantiomerically enriched secondary alcohol. The transformation benefits from a relatively stable, easily-purified reagent/product combination, and leads directly to a large number of important target molecules and/or advanced intermediates for the preparation of numerous others. One might estimate that ketone reduction accounts for somewhere in the region of 25% of all asymmetric catalysis research work.

Recent Results

Over the last three years we have developed a number of ruthenium (II) and rhodium (III) based complexes which have proven highly effective at the asymmetric catalysis of ketone reduction. These can be divided into two broad classes: i) 'transfer' hydrogenation catalysts in which the primary reductant is either an alcohol or formic acid, and ii) 'pressure' hydrogenation of ketones. Taking these in turn;

Asymmetric transfer hydrogenation catalysts: [1-4] These catalysts literally 'transfer' two atoms of hydrogen from a suitable donor to a ketone substrate. The catalysts that we have developed are represented by structures **1** and **2** in Figure **1** and have been designed based on the precedent set by Noyori et al [5,6]. The enantiomerically-pure diamine ligand component results in the formation of a chiral-at-metal structure which subsequently directs the asymmetric transformation. The link (tethering group) between the diamine part and the arene [7-10] or cyclopentadienyl ring [11] increases the stability and the activity of the catalysts. The catalysts have a similar mechanism of action (also in Figure **1**). In each case, HCl is first lost to give the 16 electron species **3** which then 'takes' two hydrogen atoms from a donor such as isopropanol or formic acid to give the hydride **4**, which in turn transfers these to a ketone substrate. This process regenerates the catalyst which then re-enters the catalyst cycle. Because the catalysts are active, loadings can be reduced to as low as 0.01 mol% (i.e. corresponding to a substrate/catalyst ratio of over 10,000:1).

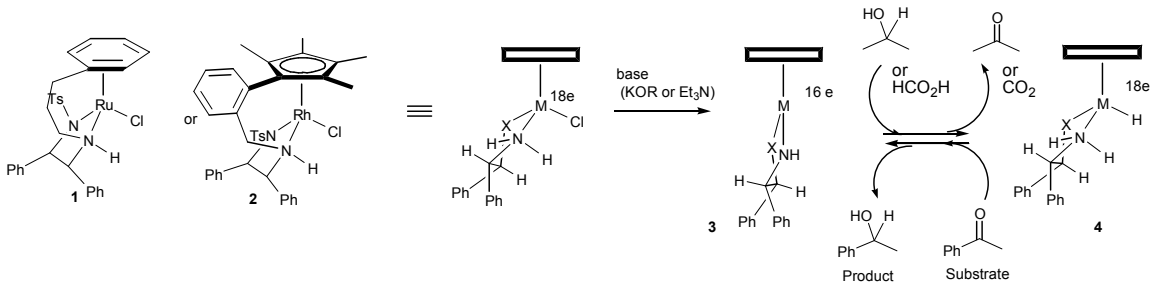

Figure 1 Structure of Ruthenium(II) and Rhodium(III) catalysts and mechanisms of action

The catalysts give a very high enantioselectivities in the reduction reaction. Using the ruthenium catalyst, aryl/alkyl ketones are particularly good substrates and can be reduced in high enantiomeric ratios. These work well because the aromatic ring of the substrate enters into a stabilising π edge/face interaction with the arene (or Cp) on the metal (Figure **2**).

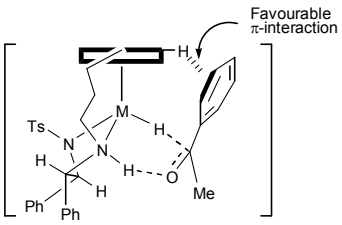

Figure 2 Asymmetric induction mechanism in transfer hydrogenation

This is effectively a 'hydrogen-bond' which can also operate through methyl substituents on the rings. Figure **3** details some of the excellent results we have obtained using catalyst **1** in ketone reductions, whilst Figure **4** illustrates products of ketone reduction with Rh(III) catalyst **2**, which works particularly well for alpha-substituted ketones[±].

Many of the target alcohols are important synthetic building blocks, and we are currently working on extending our applications to further classes of valuable target molecules in collaboration with industry and with research council support.

One of the most attractive features of the reactions, in additional to excellent green credentials, is that they can be carried out under very mild conditions; typically room temperature and pressure, and without the need for rigorous exclusion of air or moisture. In fact the reactions can even be run in aqueous solution.

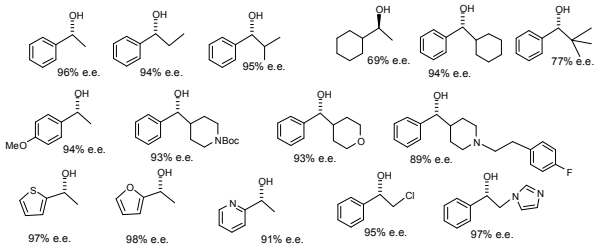

Figure 3 Examples of ketone reduction products obtained using catalyst **1** (in formic acid/trimethyamine)

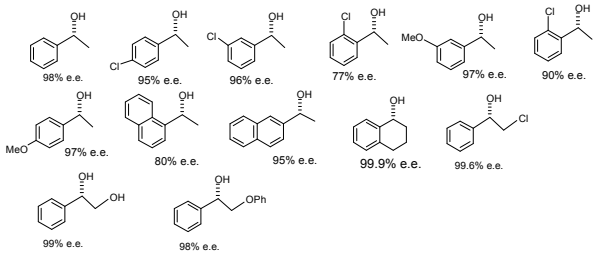

Figure 4 Examples of ketone reduction products obtained using Rhodium catalyst **2** (in formic acid/ triethyamine)

Asymmetric 'pressure' hydrogenation catalysts [12] Our catalysts for pressure hydrogenation catalyse the more conventional transfer of two hydrogen atoms from hydrogen gas to the ketone substrate. The catalysts **5** contain, as ligands, a combination of two phosphorus donors (representing a modification on the diphosphine previously used by others in similar reactions [13, 14]), a diamine and two chlorine atoms.

The mechanism of reduction involves a six-centre transition state of a type analogous to the transfer hydrogenation system described above in that first hydrogen is transferred to the catalyst and this is then in turn transferred to the substrate through a 6-centre transition state as illustrated in Figure **5** & **6** on the next page**.**

The asymmetric reduction of simple unfunctionalised ketones may be archived with full conversions and e.e.s up to 99%. The substrate to catalyst ratio is typically 2000 but sometimes as high as 10,000. The work, carried out in collaboration with Rhodia, has recently been published [15-17].

[±] note that e.e. = enantiomeric excess, a common measurement of enantiomeric purity which can be defined as %major enantiomer-%minor enantiomer, where the sum of both enantiomers is 100%.

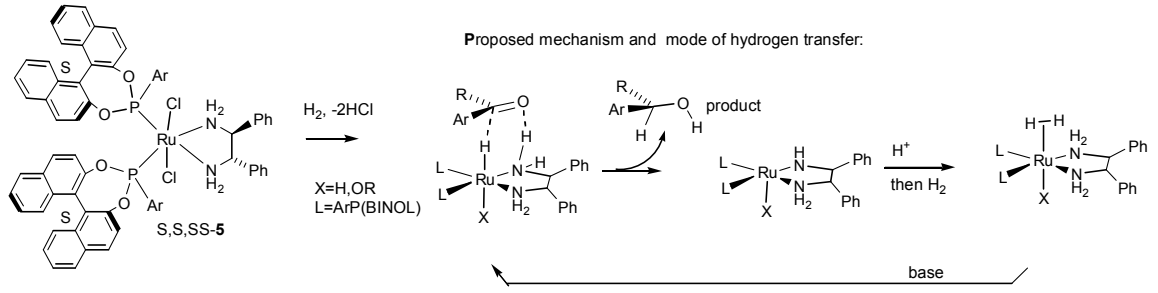

Figure 5 Asymmetric hydrogenation using Monodonor phosphine/Ru/diamine complexes

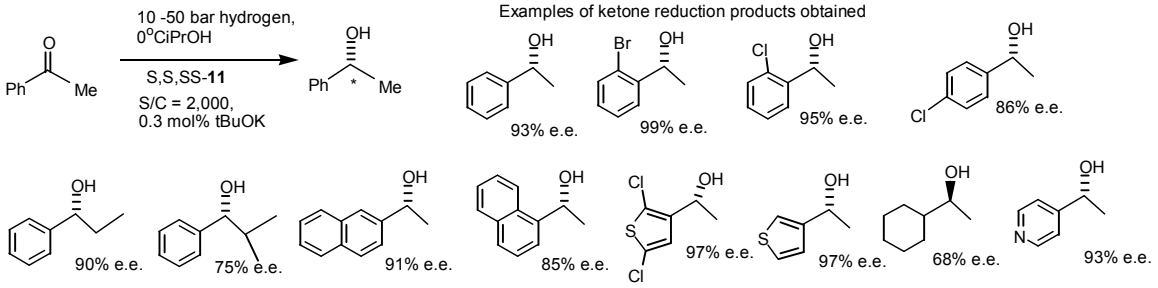

Figure 6 Asymmetric hydrogenation using monodonor phosphine/Ru(II)/DPEN complexes

Importance of the EPSRC Chemical Database Service.

The EPSRC Chemical Database Service (CDS) has been invaluable to us in the characterisation of the intermediates and ligands for these catalysts. We made use of the multi-technique spectroscopic database system SpecInfo system and were able to easily check any known structures within the Cambridge Crystallographic Database.

The reaction databases provided by the CDS were also key. In particular these include a number tailored to areas of more specialist chemistry (e.g. Protecting Groups, Solid Phase Synthesis, and Chiral Separation). The information we got from these sources complemented what were also able to obtain via the Beilstein and CAS SciFinder resources.

Without the access to the information and characterisation sources which it makes available, much of this work would not have been completed or would have taken significantly longer.

[1] Palmer, M. J.; Wills, M. *Tetrahedron: Asymmetry* **1999**, *10*, 2045.
[2]Noyori, R.; Hashiguchi, S. *Acc. Chem. Res.* **1997**, *30*, 97.
[3]Gladiali, S.; Alberico, E. *Chem. Soc. Rev.* **2006**, *35*, 226.
[4]Ikariya, T.; Murata, K.; Noyori, R. *Org. Biomol. Chem.* **2006**, *4,* 393.
[5]Fujii, A.; Hashiguchi, S.; Uematsu, N.; Ikariya, T.; Noyori, R. *J. Am. Chem. Soc.* **1996**, *118*, 2521.
[6]Haack, K. J.; Hashiguchi, S.; Fujii, A.; Ikariya, T.; Noyori, R. *Angew. Chem. Int. Ed.* **1997**, *36*, 285
[7]Hannedouche, J.; Clarkson, G.; Wills, M. *J. Am. Chem. Soc.,* 2004, **126**, 986-987.
[8]Cheung, F. K.; Hayes, A. M.; Hannedouche, J.; Yim, A. S. Y.; Wills, M. *J. Org. Chem.,* 2005, **70**, 3188 .
[9]Hayes, A. M.; Morris, D. J.; Clarkson, G. J.; Wills, M. *J. Am. Chem. Soc.* 2005, **127**, 7318.
[10]Williams, G. D.; Wade, C. E.; Wills, M. *Chem. Commun.,* 2005, 4735.
[11]Matharu, D. S.; Morris, D. J.; Kawamoto, A. M.; Clarkson, G. J.; Wills, M. *Org. Lett.,* 2005, **7**, 5489.
[12]Clapham, S. E.; Hadzovic, A.; Morris, R. H. *Coord. Chem. Rev.* **2004**, *248*, 2201.
[13]Ohkuma, T.; Koizumi, M.; Muniz, K.; Hilt, G.; Kabuto, C.; Noyori, R. *J. Am. Chem. Soc.,* 2002, **124**, 6508.
[14]Doucet, H.; Ohkuma, T.; Murata, K.; Yokozawa, T.; Kozawa, M.; Katayama, E.; England, A. F.; Ikariya, T.; Noyori, R. *Angew. Chem., Int. Ed.* 1998, **37**, 1703.
[15]Xu, Y.; Alcock, N. W.; Clarkson, G. J.; Docherty, G.; Woodward, G.; Wills, M. *Organic Letters*, 2004, **6**, 4105.
[16]Xu, Y.; North, C.; Clarkson, G. J.; Docherty, G.; Woodward, G.; Wills, M. *J. Org. Chem.,* 2005, **70**, 8079.
[17] Thayer, A. Chiral Chemistry', *Chemical and Engineering News*, Sept 5th 2005, 40-47.